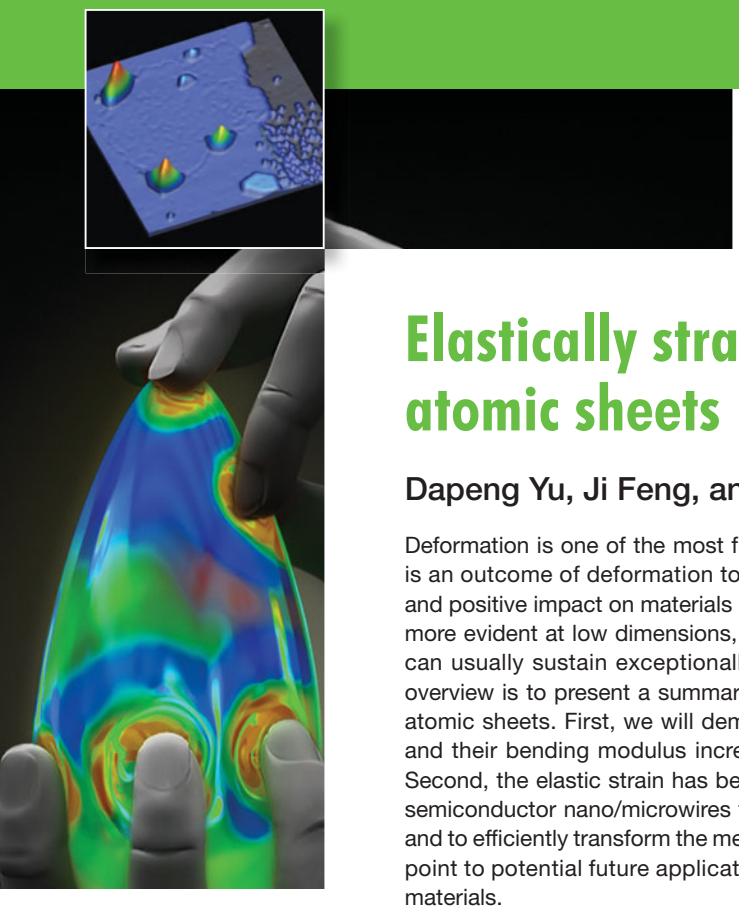


Elastically strained nanowires and atomic sheets

Dapeng Yu, Ji Feng, and James Hone

Deformation is one of the most fundamental aspects of materials. While mechanical failure is an outcome of deformation to be avoided, elastic deformation can have a pronounced and positive impact on materials properties. The effect of elastic deformation becomes even more evident at low dimensions, because at the micro/nanoscale, materials and structures can usually sustain exceptionally high elastic strains before failure. The purpose of this overview is to present a summary of recent progress on elastically strained nanowires and atomic sheets. First, we will demonstrate that nanowires can sustain large elastic strains, and their bending modulus increases exponentially as the nanowire diameter decreases. Second, the elastic strain has been found to significantly modify the electronic structure of semiconductor nano/microwires to induce a metal–insulator transition at room temperature and to efficiently transform the mechanical energy into electricity. These recent developments point to potential future applications based on the elastic strain engineering of nanoscale materials.

Introduction

Strain is a universal phenomenon pertinent to the synthesis, fabrication, and applications of all types of materials. Strain can have two distinct regimes: In the plastic regime, materials generally undergo irreversible changes, such as failure or property degradation. Elastic deformation, on the other hand, can induce reversible changes to materials properties, from electronic and chemical to optical; this is called elastic strain engineering (ESE). A particularly successful application of strain engineering is pushing the limit of miniaturization of silicon-based field-effect transistors.[1] By alternating deposition of Si and Ge layers, the interlayer lattice mismatch creates controllable strain in the silicon crystal. The precisely controlled strain breaks the crystal field symmetry and reduces the scattering of carriers by phonons, resulting in substantially increased carrier mobility, which allows for further reduction in the channel size.

"Magnified" strain effects in nanowires

The strength of a material depends very strongly on its dimensions. Typically, smaller structures can tolerate larger deformations before yielding. For a given rod structure under a bending deformation, the smaller the radius of the rod (distance to the rod axis), the larger the strain it can sustain at the maximum elastic loading stress.[2] Therefore, it is anticipated that ESE can be profitably explored in materials with reduced dimensions, such as nanowires and atomic sheets.

Rapid progress in device miniaturization has led to the quick rise of flexible, nanoscale devices for which one-dimensional nanowires and atomic sheets such as graphene are particularly promising candidate materials. These materials possess unusual electronic properties, frequently arising from giant surface effects and strong quantum confinement. Thanks to their reduced dimensions, these materials also exhibit superb mechanical properties, some of which (e.g., graphene) are among the strongest human-made materials. Moreover, unlike in strain-engineering in the conventional microelectronics industry, where uniform strain is often employed to enhance materials properties, in these low-dimensional wires and sheets, inhomogeneous strain fields can also be generated, providing unprecedented opportunities to explore paradigms of ESE. Therefore, nanowires and atomic sheets are ideal platforms to explore novel elastic strain effects and device concepts at the nanoscale.

Wong et al. were among the first to address the size effects of mechanical properties of nanotubes and SiC nanorods using atomic force microscopy (AFM).[3] They found that the strengths of SiC nanorods were substantially greater

Dapeng Yu, School of Physics, Peking University; yudp@pku.edu.cn
Ji Feng, School of Physics, Peking University; jfeng11@pku.edu.cn
James Hone, Department of Electronic Engineering, Columbia University; jh2228@columbia.edu
DOI: 10.1557/mrs.2014.6

© 2014 Materials Research Society

https://doi.org/10.1557/mrs.2014.6 Published online by Cambridge University Press

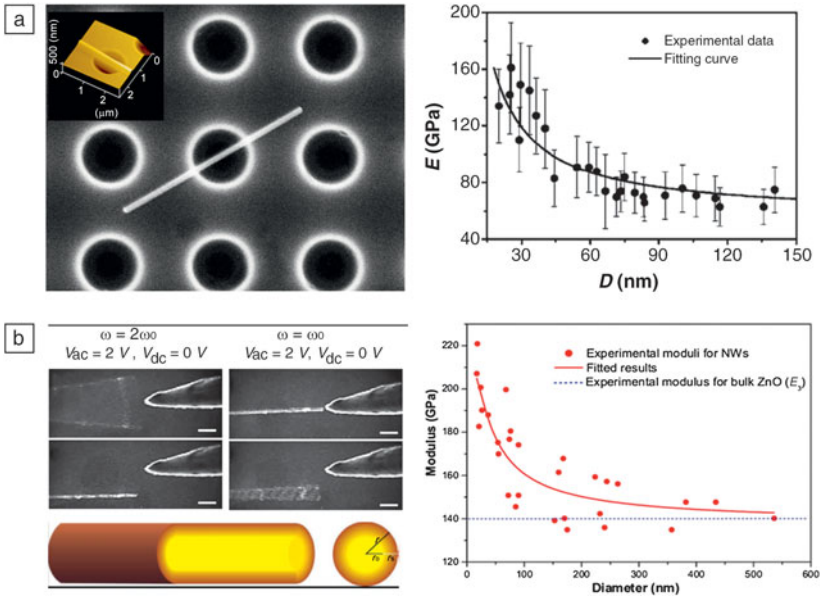


Figure 1. Sample size effects on the bending Young's modulus in (a) metallic Ag nanowires[4] and (b) ceramic zinc oxide nanowires.[5] In both cases, the modulus (*E*) increases dramatically with a decrease in the nanowire diameter (*D*).

than those found previously for SiC bulk structures. The size effect of nanowires is also reflected in the variation of the Young's modulus upon bending as a function of the nanowire diameter. Yu's group[4] systematically investigated metallic silver nanowires by precisely placing individual Ag nanowires of different diameters over microhole arrays via focused ion beam milling. A calibrated AFM tip was used to push down on the middle point of each suspended Ag nanowire. From measurement of the force applied with each push and the corresponding displacement, the bending Young's modulus could be easily deduced, as shown in **Figure 1**. It is somewhat surprising to observe that the bending Young's modulus increases from the bulk value of ~76 GPa to as high as ~160 GPa as the diameter of the nanowire decreases to ~20 nm. Similar observations were found for other brittle ceramic materials. For example, Zhu and co-workers[5] studied ZnO nanowires by applying an alternating electric field at the tip of a single ZnO nanowire, causing it to undergo bending vibrations (Figure 1b). The bending Young's modulus increased exponentially with decreasing ZnO nanowire diameter, from the bulk value of ~140 GPa to ~200 GPa at a diameter of 20 nm. A core–shell model was proposed to explain the abnormal increase.

Han and Zhang carried out a systematic investigation of the mechanical properties of a series of semiconducting nanowires (Si, SiC, and glassy silicon oxide, which are all brittle in bulk form).[6–9] The size-dependence of the energy bandgap of ZnO nanowires under elastic tensile strain is particularly interesting, observed via *in situ* cathodoluminescence measurements in a scanning electron microscope (SEM). They found that the maximal strain and the corresponding bandgap modification increased with decreasing nanowire diameter.[10] For example, the bandgap energy decreased (was red-shifted) by about 110 meV for a smaller nanowire ~100 nm in diameter under a large elastic tensile strain up to ~7.3%, which is nearly double the value of ~59 meV for a larger nanowire of 760 nm in diameter under a tensile strain of 1.7%. A two-step linear feature involving bandgap reduction caused by strain and a corresponding critical strain was observed in ZnO nanowires with diameters <300 nm. The same group also observed unusually large elastic strains in copper nanowires approaching the theoretic elastic limit of bulk copper.[11]

Such large elastic strains can be used to tune other properties of nanowires, as there is a strong mechanoelectrical coupling. For example, the conductance of ZnO nanowires and CdSe nanobelts (ribbon-like structures) increases very sensitively with the increase in bending strain under AFM tip manipulation.[12] Yu's group conducted a systematic investigation of strain modulation on the optical emission energy and electronic fine structures of ZnO nano/microwires under elastic bending deformation.[13–16] To confirm that the bending deformation is in the elastic regime, a single ZnO nanowire was pushed and bent on a silicon substrate, before applying a drop of liquid to release the bent nanowire from the substrate and return it to its original straight form. The bending strain modifies the near-edge emission energy of ZnO nanowires, as revealed by cathodoluminescence (CL) spectroscopy at liquid nitrogen temperature (~81 K). **Figure 2** presents a collection of CL spectra along the axial positions of a single ZnO nanowire bent into an "L" shape. These were obtained from 13 axial

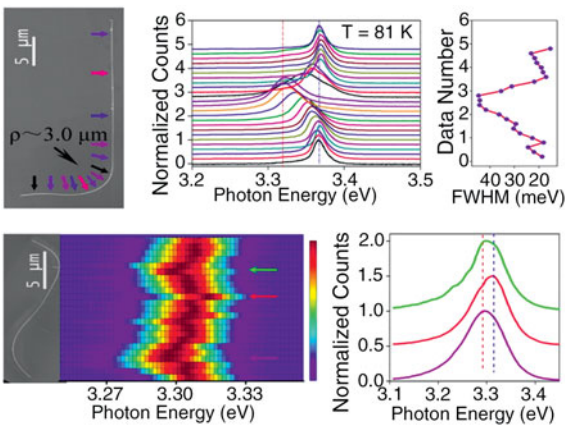


Figure 2. Elastic strain modification of the emission energy of cathodoluminescence of a bent ZnO nanowire. Evidence of elastic bending strain modification on the optical properties of bent ZnO nanowires via high spatial/energy resolution cathodoluminescence (CL) at 81 K. CL spectra correspond to locations along the nanowires bent into L- and S-shapes.[13]

https://doi.org/10.1557/mrs.2014.6 Published online by Cambridge University Press

positions corresponding to different radii of bending curvature (and different bending strains).[13] Clearly, the energy of the near-edge emission is altered by the changing bending strain, resulting in an overall red-shift with increasing strain. A ZnO nanowire bent into an "S" shape displays similar red-shifting at the two bent positions (maximum strains).[13] Obvious peak broadening is also observed.

Considering the electron beam scattering volume at the working accelerating voltage and the exciton diffusion length, wires of larger diameters would allow better resolution of the strain modification route for the optical properties of ZnO. As shown in **Figure 3**, a hexagonal-shaped ZnO microwire, with a diameter ~3 μm and length of several hundreds of μm, was used for systematic analysis.[14] Nine positions marked with "I" to "IX" were selected for a CL line scan analysis along the radial direction. Because at each position the wire has a different bending radius of curvature, it undergoes different elastic bending strains. Across the cross-section at each line scan position, there exists a linear strain ranging from tensile to compressive. Clearly, the two free ends marked "I" and "IX" are strain-free. To present the change rate of the local strain along the axial direction, a novel parameter called the strain gradient β is proposed, which is defined as the inverse of the radius ρ of the bending curvature: $\beta = 1/\rho$. With a scan step ~100 nm, more than 30 CL spectra were collected along the cross-section at each line-scan position. The complete sets of the CL spectra collected at the nine positions are presented in Figure 3, and the corresponding strain gradients are marked as well. The two dominant exciton peaks shift linearly with the strain gradient.[14]

CL spectroscopy in the SEM not only guarantees very high spatial resolution compared to laser excitation but also has high energy resolution at low temperature, allowing for the collection of very clean spectra that make the subsequent analysis much more straightforward. Therefore, a systematic CL spectroscopy analysis was conducted at liquid helium temperature (~5.4 K), as shown in Figure 3.[15] A representative series of CL spectra are presented that were obtained from a line scan along the cross-sectional direction of another bent ZnO microwire. Surprisingly, modification of the bending strain is asymmetric, that is, at the tensile side, a mono red-shift with an increase in the tensile strain can be seen. However, on the compressive side, blue-shifting, broadening, and peak splitting occur with increasing compressive strain. Such a strain gradient effect is unique and representative for nanowire structures under non-uniform bending deformation, as the strain gradient causes a built-in field that can manipulate the transport of the carriers, leading to possible new concept devices.

Elastic strain also has significant effects on other functional properties of the nanowires.[16–20] Yang et al. investigated

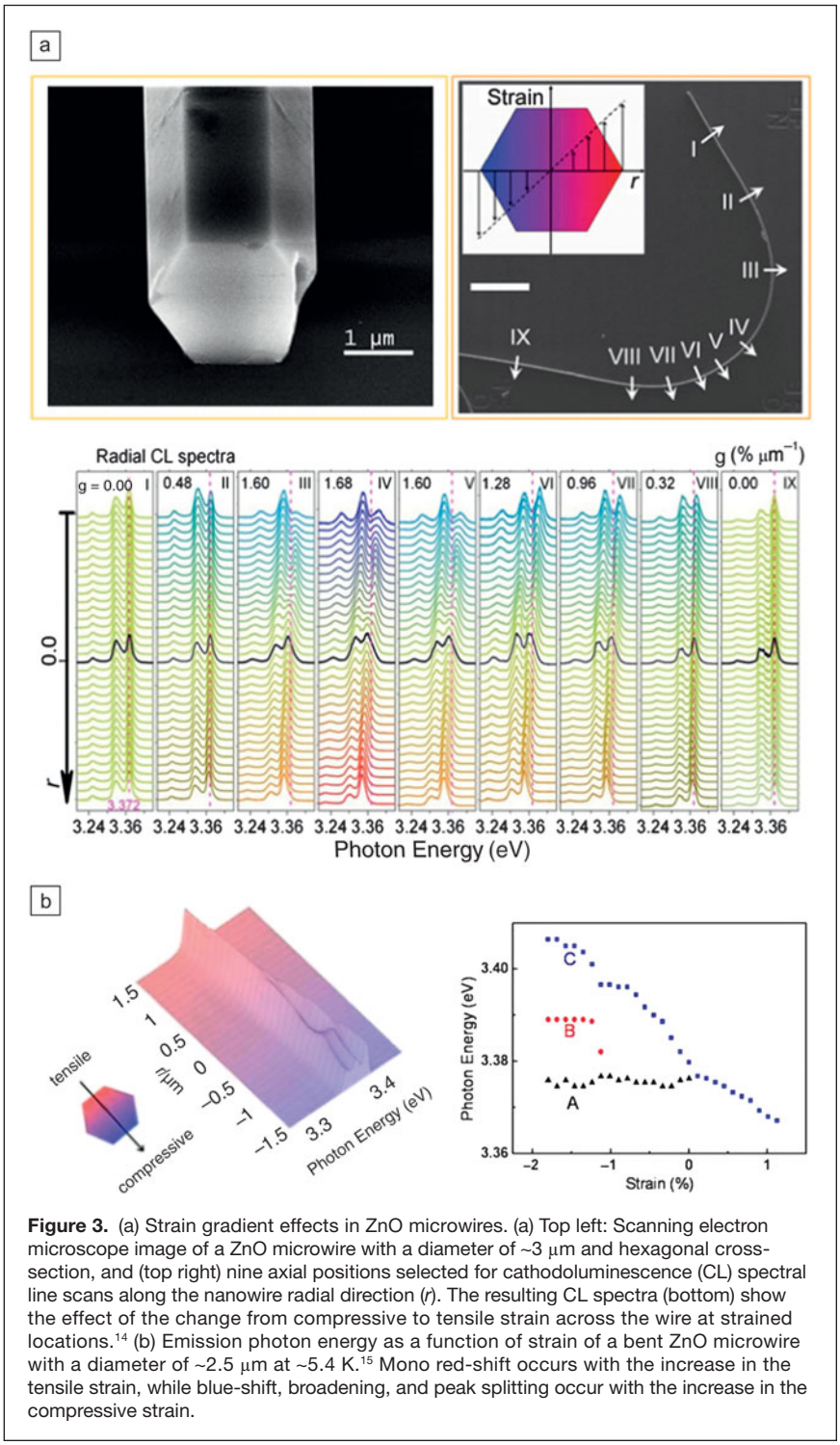


Figure 3. (a) Strain gradient effects in ZnO microwires. (a) Top left: Scanning electron microscope image of a ZnO microwire with a diameter of ~3 μm and hexagonal cross-section, and (top right) nine axial positions selected for cathodoluminescence (CL) spectral line scans along the nanowire radial direction (*r*). The resulting CL spectra (bottom) show the effect of the change from compressive to tensile strain across the wire at strained locations.[14] (b) Emission photon energy as a function of strain of a bent ZnO microwire with a diameter of ~2.5 μm at ~5.4 K.[15] Mono red-shift occurs with the increase in the tensile strain, while blue-shift, broadening, and peak splitting occur with the increase in the compressive strain.

https://doi.org/10.1557/mrs.2014.6 Published online by Cambridge University Press

the piezoresistance of a single *p*-silicon nanowire under uniaxial tensile/compressive strain and observed a so-called giant piezoresistance phenomenon.[16] Liu et al. theoretically constructed an elastically strained silicon nanoribbon, which consists of a normal and a strained unit cell, called a single-element electronic heterojunction superlattice.[18] In such a strained configuration, it is predicted that, due to the strain effect and quantum confinement, it is possible to manipulate the motion of carriers via elastic strain.

Wu et al. demonstrated another excellent example of elastic strain manipulation of nanowire properties.[20] Via simple tip manipulation of the bending deformation of a single-crystal vanadium dioxide nanowire, they were able to control the metal–insulator transition at room temperature, which normally happens at an elevated temperature in its bulk counterpart, as shown in **Figure 4**.

Wang's group at the Georgia Institute of Technology has used the elastic bending deformation of ZnO micro/nanowires to create new kinds of nanogenerators[21–26] and flexible strain sensors.[27,28] **Figure 5** summarizes the main physical principle as to how elastic bending strain converts mechanical energy into electricity using piezoelectric ZnO nanowires. The initial nanogenerators are based on a tungsten AFM tip bending vertically arrayed ZnO nanowires, and the output arises from the unique coupling of piezoelectric and semiconducting properties. It is found that a metal (tungsten tip)-semiconductor (ZnO nanowires) Schottky barrier plays a crucial role and governs the whole power generating process. Specifically, no output current is collected when the tungsten tip first touches the nanowire and pushes the nanowire, and power output occurs only when the tip touches the compressive side of the bent nanowire. So far, flexible high-output nanogenerators based on ZnO nanowire arrays have already been demonstrated that can charge light-emitting diodes[25] and could potentially be used in wireless microelectronic devices.[27] The excellent mechanical and strain-enhanced physical properties have made semiconductor nanowires competitive and promising candidates for use in flexible solar cells[29] and supercapacitors.[30]

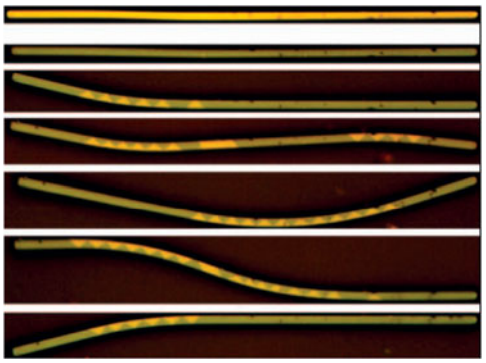


Figure 4. Elastic bending strain manipulation of metal (bright contrast)–insulator (dark contrast) transition at room temperature in VO_2 nanowires.[20]

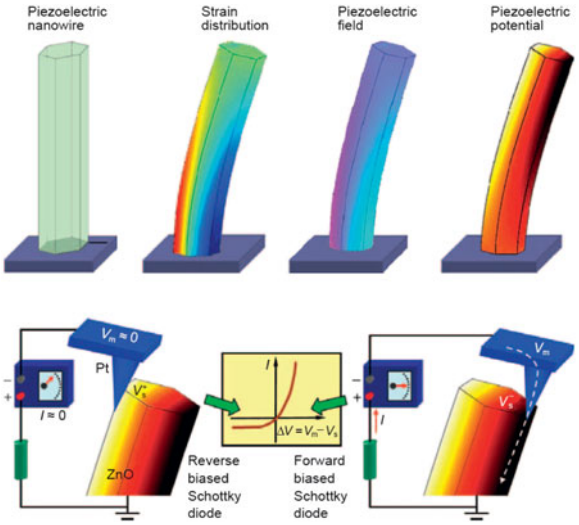


Figure 5. Nanowire nanogenerators based on piezoelectric ZnO nanowires: Elastic bending strain transfers mechanical energy into electricity, revealing a unique coupling of piezoelectric and semiconducting properties in a metal-semiconductor Schottky barrier governed transport process. V_m, potential at the metal tip; V_s, potential at the nanowire; I, current.[21–25,27]

Graphene, the strongest material

Graphene is a two-dimensional atomic carbon sheet that displays remarkable and distinctive electronic and mechanical properties[31–33] (see the December 2012 issue of *MRS Bulletin*). Its unique electronic properties, which arise from a linear Dirac-like band dispersion near the Fermi level, have led to novel physics and have stimulated intensive investigations into high mobility all-carbon electronics. Because graphene consists of a two-dimensional sheet of covalently bonded carbon atoms, its intrinsic tensile strength is predicted to exceed that of any other material. This enormous strength is the motivation for the current use of carbon-fiber reinforcements, whose strength still falls well short of the intrinsic value of the fibers, in advanced composites. Replacement or supplementation with graphene may permit even higher performance composite materials.

Lee et al. experimentally verified the ultrahigh strength of graphene.[34] As shown in **Figure 6**, the elastic properties and intrinsic breaking strength of freestanding monolayer graphene membranes were studied by nano-indentation using AFM. Analysis of the shape of the force-displacement curves yields a Young's modulus of ~1 TPa, equivalent to the basal-plane stiffness of graphite—as expected due to the weak interlayer interaction. To deduce the breaking strength from the measured breaking force, finite element analysis simulated the experiment, employing a nonlinear constitutive model of the stress–strain behavior. The simplest such model yields an intrinsic strength of 130 GPa. Subsequent analysis employing a more detailed nonlinear anisotropic model yielded a more accurate value of 100 GPa from the same data.[35] This ultrahigh strength demonstrates that graphene is the strongest material

https://doi.org/10.1557/mrs.2014.6 Published online by Cambridge University Press

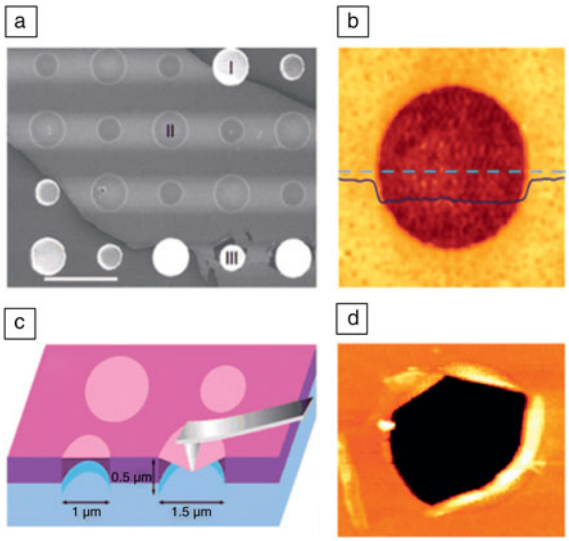


Figure 6. Elastic properties and intrinsic breaking strength of freestanding monolayer graphene membranes suspended on microholes by atomic force microscope (AFM) nanoindentation.[34] The schematic (c) depicts how force is applied with the AFM tip, and scanning electron microscopy (a) and AFM images ((b) intact and (d) fractured) show the graphene before and after measurements. (a) I is a hole without graphene; II is a hole with graphene; and III is broken graphene.

ever measured, and shows that atomically perfect nanoscale materials can be mechanically tested to deformations well beyond the linear regime. In more recent work, Lee et al. have demonstrated that this ultrahigh strength is maintained even in the presence of grain boundaries, opening up the possibility of large-area applications.[36]

The ultrahigh mechanical strength makes it possible to impart very large elastic strains, which can significantly engineer the electronic states of graphene.[37–39] In particular, strain causes shifts in the location of the Dirac points in the electronic band structure in the same way as an applied magnetic field. A particularly dramatic example of this effect was demonstrated by Levy and co-workers on highly strained nanobubbles in graphene grown on a Pt(111) substrate, as shown in **Figure 7**. Via detailed measurements and simulation of the scanning tunneling spectra, they found that the bending strain of the bubbled graphene caused enormous pseudo-magnetic fields greater than 300 Tesla, resulting in quantized Landau levels.[39] These results[34,39] suggest that strain engineering at nanoscale energy levels can be a viable means to control the electronic structure of graphene even at room temperature. The experimental demonstration of the enormous pseudo–magnetic fields also provides a new basis to study the charge carriers in previously inaccessible extremely high magnetic field

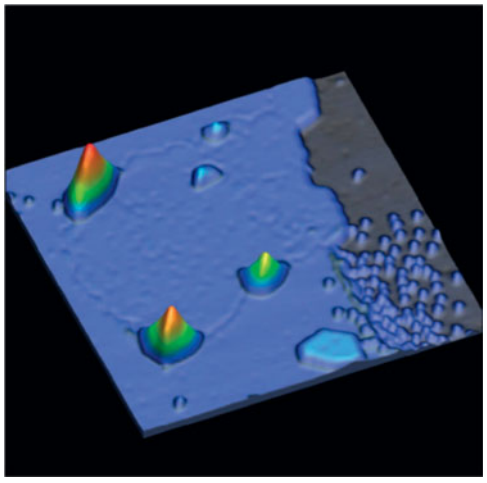


Figure 7. Demonstration by scanning tunneling microscopy of quantized Landau levels occurring in bubbled graphene—a result of strain-induced pseudo-magnetic fields greater than 300 T.[39]

regimes in condensed matter and to achieve deliberate mechanical control over electronic structure in graphene.

Feng et al.[40,41] presented a recent example demonstrating strain engineering of an atomic sheet. They considered the possibility of tuning the optical absorption and charge carrier dynamics in an atomically thin semiconducting membrane. The central idea proposed is to utilize the spatial variation of the bandgap induced by the elastic strain field to direct the flow of charge carriers and create a spatial concentration of excitons or charge carriers. Using this idea, a photovoltaic device that is made from a strain-engineered MoS_2 monolayer was proposed. As shown in **Figure 8**, the atomic sheet is subject to a central load configuration under a mechanical indenter, whereupon an inhomogeneous strain field is focused toward the center of the membrane. The strain field thus

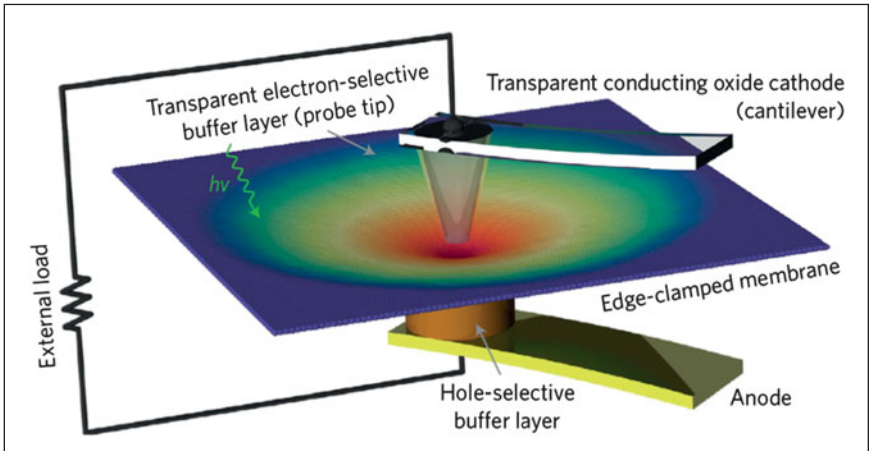


Figure 8. Strain-engineered artificial atom as a broad-spectrum solar energy funnel. Mechanical indentation of a monolayer sheet of MoS_2 creates a strain gradient and corresponding variation in bandgap, resulting in broad spectrum absorption and funneling of charge carriers to the indentation site.[40]

https://doi.org/10.1557/mrs.2014.6 Published online by Cambridge University Press

produced then modulates the exciton spectrum of the semiconductor to create an effective built-in field, concentrating the charge carriers toward the center of the funnel-shaped device. Feng et al. proposed that a strain-engineered funnel device will capture and concentrate a broad range of the solar spectrum as schematically shown in Figure 8. Very recently, using photoluminescence imaging, a strain-induced reduction of the direct bandgap and funneling of photo-generated excitons toward regions of higher strain was experimentally observed in MoS_2 monolayers.[42] In another experiment, Nam et al. induced a strain gradient along Ge nanowires to induce charge carrier concentration similar to conventional semiconductor heterostructure. This effect was probed by spatially resolved photoluminescence measurements.[43]

Summary and outlook

Semiconductor nanowires and graphene are representative 1D and 2D nanostructures, respectively, which can tolerate much higher elastic deformation compared to their bulk counterparts. Just as classical chemical doping allows for the fabrication of a wide range of optoelectronic devices, such as photovoltaic cells, semiconductor lasers, light-emitting diodes, and field-effect transistors, elastic strain offers another degree of freedom to continuously and reversibly tune the lattice parameter in nanowires and atomic sheets, and to modulate the electronic states and even carrier dynamics. We would like to point out that although there has been exciting progress already made in the elastic strain engineering of nanowires and atomic sheets, many challenges remain in this field. Innovative ideas, novel means of characterization, and more powerful and effective methods of theoretical calculations and simulations are needed before the dream of new concept strain-modulated nanodevices is realized and changes our daily lives.

Acknowledgments

This work is supported by NSFC (11174009) and the National 973 Programs of China (2013CB921900, 2012CB619402).

References

1. M. Ieong, B. Doris, J. Kedzierski, K. Rim, M. Yang, *Science* **306**, 2057 (2004).
2. P. Hiralal, H.E. Unalan, G.A.J. Amaratunga, *Nanotechnology* **23**, 194002 (2012).
3. E.W. Wong, P.E. Sheehan, C.M. Lieber, *Science* **277**, 1971 (1997).
4. G.Y. Jing, H.L. Duan, X.M. Sun, Z.S. Zhang, J. Xu, Y.D. Li, J.X. Wang, D.P. Yu, *Phys. Rev. B* **73**, 235409 (2006).
5. C.Q. Chen, Y. Shi, Y.S. Zhang, J. Zhu, Y.J. Yan, *Phys. Rev. Lett.* **96**, 075505 (2006).
6. X.D. Han, Y.F. Zhang, K. Zheng, X.N. Zhang, Z. Zhang, Y.J. Hao, X.Y. Guo, J. Yuan, Z.L. Wang, *Nano Lett.* **7**, 452 (2007).
7. X. Han, S. Zheng, Y. Zhang, K. Zheng, X. Liu, G. Chen, Y. Hao, X. Guo, *Nano Lett.* **8**, 2258 (2008).
8. K. Zheng, X. Han, L. Wang, Y. Yue, Y. Zhang, Y. Qin, X. Zhang, Z. Zhang, *Nano Lett.* **9**, 2471 (2009).
9. K. Zheng, C. Wang, Y.-Q. Cheng, Y. Yue, X. Han, Z. Zhang, Z. Shan, S.X. Mao, M. Ye, Y. Yin, E. Ma, *Nat. Commun.* **1**, 24 (2010).
10. B. Wei, K. Zheng, Y. Ji, Y. Zhang, Z. Zhang, X. Han, *Nano Lett.* **12**, 4595 (2012).
11. Y. Yue, P. Liu, Z. Zhang, X. Han, E. Ma, *Nano Lett.* **11**, 3151 (2011).
12. X.B. Han, G.Y. Jing, X.Z. Zhang, R. Ma, X. Song, J. Xu, Z. Liao, N. Wang, D. Yu, *Nano Res.* **2**, 553 (2009).
13. X.B. Han, L.Z. Kou, X.L. Lang, J.B. Xia, N. Wang, R. Qin, J. Lu, J. Xu, Z.M. Liao, X.Z. Zhang, X.D. Shan, X.F. Song, J.Y. Gao, W.L. Guo, D.P. Yu, *Adv. Mater.* **21**, 4937 (2009).
14. X. Han, L. Kou, Z. Zhang, Z. Zhang, X. Zhu, J. Xu, Z. Liao, W. Guo, D. Yu, *Adv. Mater.* **24**, 4707 (2012).
15. Z.M. Liao, H.C. Wu, Q. Fu, X. Fu, X. Zhu, J. Xu, I.V. Shvets, Z. Zhang, W. Guo, Y. Leprince-Wang, Q. Zhao, X. Wu, D.P. Yu, *Sci. Rep.* **2**, 452 (2012).
16. R.H. He, P.D. Yang, *Nat. Nanotechnol.* **1**, 42 (2006).
17. J.S. Milne, A.C.H. Rowe, S. Arscott, *Phys. Rev. Lett.* **105**, 226802 (2010).
18. Z. Liu, J. Wu, W.H. Duan, M.G. Lagally, F. Liu, *Phys. Rev. Lett.* **105**, 016802 (2010).
19. A.M. Smith, A.M. Mohs, S. Nie, *Nat. Nanotechnol.* **4**, 56 (2008).
20. J. Cao, E. Ertekin, V. Srinivasan, W. Fan, S. Huang, H. Zheng, J.W.L. Yim, D.R. Khanal, D.F. Ogletree, J. Wu, *Nat. Nanotechnol.* **13**, 132 (2009).
21. Z.L. Wang, J.H. Song, *Science* **312**, 242 (2006).
22. Z.L. Wang, *Nano Res.* **1**, 1 (2008).
23. X.D. Wang, J.H. Song, J. Liu, Z.L. Wang, *Science* **316**, 102 (2007).
24 Y. Qin, X. Wang, Z.L. Wang, *Nature* **451**, 908 (2008).
25. G. Zhu, R.S. Yang, S.H. Wang, Z.L. Wang, *Nano Lett.* **10**, 3151 (2010).
26. S. Xu, B.J. Hansen, Z.L. Wang, *Nat. Commun.* **1**, 93 (2010).
27. J. Zhou, Y.D. Gu, P. Fei, W.J. Mai, Y.F. Gao, R.S. Yang, G. Bao, Z.L. Wang, *Nano Lett.* **8**, 3035 (2008).
28. Q. Yang, W.H. Wang, S. Xu, Z.L. Wang, *Nano Lett.* **11**, 4012 (2011).
29. W. Wang, Q. Zhao, H. Li, H. Wu, D. Zou, D. Yu, *Adv. Funct. Mater.* **22**, 2775 (2012).
30. H. Li, Q. Zhao, W. Wang, H. Dong, D.S. Xu, G.J. Zou, H.L. Duan, D.P. Yu, *Nano Lett.* **13**, 1271 (2013).
31. K.S. Novoselov, A.K. Geim, S.V. Morozov, D. Jiang, Y. Zhang, S.V. Dubonos, I.V. Grigorieva, A.A. Firsov, *Science* **306**, 666 (2004).
32. K.S. Novoselov, A.K. Geim, S.V. Morozov, D. Jiang, M.I. Katsnelson, I.V. Grigorieva, S.V. Dubonos, A.A. Firsov, *Nature* **438**, 197 (2005).
33. Y.B. Zhang, Y.W. Tan, H.L. Stormer, P. Kim, *Nature* **438**, 201 (2005).
34. C. Lee, X. Wei, J.W. Kysar, J. Hone, *Science* **321**, 385 (2008).
35. X. Wei, B. Fragneaud, C.A. Marianetti, J.W. Kysar, *Phys. Rev. B* **80**, 205407 (2009).
36. G.-H. Lee, R.C. Cooper, S.J. An, S. Lee, A. van der Zande, N. Petrone, A.G. Hammerberg, C. Lee, B. Crawford, W. Oliver, J.W. Kysar, J. Hone, *Science* **340**, 1073 (2013).
37. V. Pereira, A. Castro Neto, *Phys. Rev. Lett.* **103**, 046801 (2009).
38. M. Huang, H. Yan, T.F. Heinz, J. Hone, *Nano Lett.* **10**, 4074 (2010).
39. N. Levy, S.A. Burke, K.L. Meaker, M. Panlasigui, A. Zettl, F. Guinea, A.H. Castro Neto, M.F. Crommie, *Science* **329**, 544 (2010).
40. J. Feng, X. Qian, C.W. Huang, J. Li, *Nat. Photonics* **6**, 866 (2012).
41. A. Van der Zande, J. Hone, *Nat. Photonics* **6**, 804 (2012).
42. A. Castellanos-Gomez, R. Roldán, E. Cappelluti, M. Buscema, F. Guinea, H.S. J. van der Zant, G.A. Steele, *Nano Lett.* **13** (11), 5361 (2013).
43. D. Nam, D.S. Sukhdeo, J.-H. Kang, J. Petykiewicz, J.H. Lee, W. Shik Jung, J. Vučković, M.L. Brongersma, K.C. Saraswat, *Nano Lett.* **13** (7), 3118 (2013). □



https://doi.org/10.1557/mrs.2014.6 Published online by Cambridge University Press